Fuzzy Sliding Mode Control with Moving Sliding Surface of Rotary Inverted Pendulum

Muhammet Aydın[1,*], Oğuz Yakut[1]

[1] Department of Mechatronics Engineering, Faculty of Engineering, Firat University, Elazığ, Türkiye

Abstract − In this study, considering the dynamic equations of the rotary inverted pendulum system and the motor dynamics, pendulum angle is controlled with fuzzy logic sliding mode control method which has moving sliding surface using state variables in Matlab program. The sliding surface of sliding mode control method is selected as moving. A fuzzy logic structure is used to calculate the slope of slip surface. The boundary values of the membership functions in the fuzzy logic structure have been optimized using genetic algorithm codes in Matlab program. The sum of the squares of the errors is preferred as the objective function. Inputs of the fuzzy logic structure are the error of the pendulum angle and the derivative of pendulum angle error. In the fuzzy logic structure, the slope of sliding surface of sliding mode control structure is obtained as an output. From the results, it was seen that the pendulum angle reached the desired reference value around the first second and the error was approximately zero. In addition, it has been observed that the motor torque value is at the levels of 20 Nm and the motor current value is at the levels of 3 ampers. It has been obtained from the results that the motor values are at reasonable levels close to the values in practical applications. When the motor is selected according to these obtained values, there won't be a problem with the implementation of this control method in real-time applications of the rotary inverted pendulum system.

Keywords − *Fuzzy logic control, genetic algorithm, motor model, moving sliding mode control, rotary inverted pendulum, sliding surface*

1. Introduction

Due to its difficult controllability, inverted pendulum systems are one of the preferred systems in the application of control techniques. The single pendulum on a cart (Bugeja,2003) and single rotary inverted pendulum systems (Stimac, 1999), double pendulum on a cart (Zhong & Röck, 2001), and double rotary inverted pendulum systems are some of the inverted pendu-lum systems developed until today (Krishen & Becerra, 2006; Awtar, S., King, N., Allen, T. & et all, 2002).

One of the preferred inverted pendulum systems in applications is rotary inverted pendulum (rip) system. The Rip system is an excellent test system for working on the control of indirectly driven nonlinear unstable systems. The rip system has been the system of choice for control applications in recent years, where it is more manufacturable and easier to use according to an inverted pendulum on a cart. The rip system has two arms, a horizontally moving rotary arm, and a vertically moving pendulum. Rotary arm takes its motion from DC motor. After the DC motor moves the rotating arm, the pendulum connected to the rotating arm is tried to be stabilized at the upper balance point, that is, where it is unstable (Yan,2003; Kuo, Huang, & Hong 2009).

[1] muhammeta@firat.edu.tr
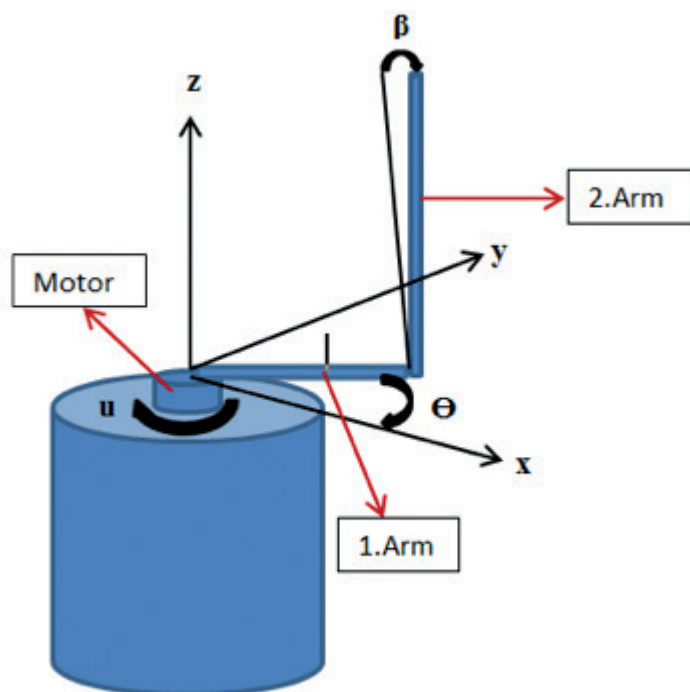
[2] oyakut@firat.edu.tr

*Corresponding Author

Figure 1. Rotary Inverted Pendulum System

In the studies presented so far in the literature for the angle control of the rotary inverted pendulum system shown in figure 1, classical control methods such as PID (Kuo, Huang, & Hong 2009), PI, PD (Altinoz, Yilmaz, & Weber, 2010), adaptive control methods with sliding mode control (Wang, 2009; Bogdanov, 2004; Aydin, Yakut, & Tutumlu, 2019), fuzzy control (Krishen & Becerra, 2006), sliding mode control (Khanesar, Teshnehlab, & Shoorehdeli, 2007), particle swarm optimization based PID control (Hassanzadeh & Mobayen, 2008; Bogdanov, 2004; Sugie & Fujimoto 1998; Sukontanakarn & Parnichkun 2009) and there are control studies sliding mode control methods via artificial neural network (Aydin, Yakut, & Tutumlu, 2019).

Especially in recent years, development of a Neuro-Fuzzy Friction Estimation Model used to estimate the joint friction coefficients of a Triple Link Rotary Inverted Pendulum system (Hazem, Fotuhi, & Bingül, 2020), controlled of a rotary inverted pendulum by adaptive techniques (Nath & Dewan, 2017) , performing stability control of double link rotary inverted pendulum with Fuzzy-LQR and Fuzzy-LQG methods (Hazem, Fotuhi, & Bingül, 2020), developing of a fuzzy logic controller for rotary inverted pendulum (Le, Vo, Van & et all, 2018) , controlling the rotary inverted pendulum with incremental sliding mode control (Hong, Nguyen, Hoang & et all 2019), a comparative analysis of the linear quadratic regulator and sliding mode control results for the rotary inverted pendulum (Nath & Dewan, 2018), performing of model-free sliding mode stabilizing control of the real rotary inverted pendulum (Yiğit, 2017), developing of numerical design method by using nonlinear sliding mode control method for Rotary inverted pendulum (Cui, 2019), comparing the PID and sliding mode control results of the rotary inverted pendulum system using PLC (Howimanporn, Chookaew & Silawatchananai, 2020), pole placement controller applied to rotary inverted pendulum system (Muñoz-Poblete, 2018), per-forming of a rotary inverted pendulum real-time stability control using an LQR-based sliding mode controller (Chawla & Singla, 2021), performing of an adaptive neural network-based control of the rotary inverted pendulum with oscillation compensation (Zabihifar, Yushchenko & Navvabi, 2020) studies have come to the fore.

In this paper, the non-linear model of the rotary inverted pendulum system was obtained and the fuzzy sliding mode control approach, which has a moving sliding surface, was used to control the pendulum. The slope of the slip surface was obtained using a fuzzy logic structure. The values of the coefficients in the fuzzy logic structure are optimized using the genetic algorithm. In the second part, Material and method, Modeling of Rotary Inverted Pendulum System and Sliding Surface Moving Fuzzy Sliding Mode Control

Design are explained. In the third chapter, results and discussion are given. In the last section, the results are mentioned.

2. Materials and Methods

2.1 Modeling of Rotary Inverted Pendulum System

The system in figure 1 is a two-degree-of-freedom system driven by a single motor. Ѳ and β are variable parameters of the system. The coordinate axis layout of the system is shown in figure 1. If the total kinetic energy of the system is calculated according to this coordinate axis set;

$$T = \frac{1}{2}m_1(\dot{x}_1^2 + \dot{y}_1^2) + \frac{1}{2}I_1\dot{\theta}^2 + \frac{1}{2}m_2(\dot{x}_2^2 + \dot{y}_2^2 + \dot{z}_2^2) + \frac{1}{2}I_2\dot{\beta}^2 \qquad (2.1)$$

x_1, y_1 in the equations are the center of gravity coordinates of the first limb., x_2, y_2 and z_2 represent the center of gravity coordinates of the second arm. m_1 and m_2 are the masses of each arm. I_1 and I_2 represent the mass moments of inertia of the arms. The limb dimensions according to their center of gravity are L_1 and L_2, respectively. The friction coefficients at the joints are b_1 and b_2. τ represents the control torque applied by the motor.

The equations of the expressions given in equation 2.1 are obtained as follows (see 2.2, 2.3, 2.4, 2.5 and 2.6).

$$x_1 = L_1 cos\theta \qquad (2.2)$$
$$y_1 = L_1 sin\theta \qquad (2.3)$$
$$x_2 = x_1 - L_2 sin\beta sin\theta \qquad (2.4)$$
$$y_2 = y_1 + L_2 sin\beta cos\theta \qquad (2.5)$$
$$z_2 = L_2 cos\beta \qquad (2.6)$$

If the above expressions are substituted to find the total kinetic energy of the system (see 2.7);

$$T = \frac{1}{2}m_1L_1^2\dot{\theta}^2 + \frac{1}{2}I_1\dot{\theta}^2 + \frac{1}{2}m_2(L_1\dot{\theta}^2 + 2L_1L_2cos\beta\dot{\theta}\dot{\beta} + L_2^2\dot{\beta}^2 + L_2^2sin^2\beta\dot{\theta}^2) + \frac{1}{2}I_2\dot{\beta}^2 \qquad (2.7)$$

Potential energy of the system (see 2.8 and 2.9):

$$V = m_2 g z_2 \qquad (2.8)$$
$$V = m_2 g L_2 cos\beta \qquad (2.9)$$

From here, the Lagrangian function is created as follows (see 2.10 and 2.11).

$$L = T - V \qquad (2.10)$$
$$L = \frac{1}{2}(m_1L_1^2 + I_1)\dot{\theta}^2 + \frac{1}{2}m_2[(L_1 + L_2^2sin^2\beta)\dot{\theta}^2 + 2L_1L_2cos\beta\dot{\theta}\dot{\beta} + L_2^2\dot{\beta}^2] + \frac{1}{2}I_2\dot{\beta}^2 - m_2gL_2cos\beta$$
$$(2.11)$$

The equation of motion for θ (see 2.12):

$$\frac{d}{dt}\left(\frac{\partial L}{\partial \dot{\theta}}\right) - \frac{\partial L}{\partial \theta} = Q_\theta \qquad (2.12)$$

If the expressions in this equation are calculated and replaced, the equation of motion for θ is obtained as follows (see 2.13).

$$\left(m_1 L_1{}^2 + I_1 + m_2 L_1 + m_2 L_2{}^2 sin^2\beta\right)\ddot\theta + m_2 L_1 L_2 cos\beta\ddot\beta - m_2 L_1 L_2 sin\beta\dot\beta^2 + 2m_2 L_2{}^2 sin\beta cos\beta\dot\beta\dot\theta = \tau - b_1\dot\theta$$

(2.13)

The equation of motion for β (see 2.14):

$$\frac{d}{dt}\left(\frac{\partial L}{\partial\dot\beta}\right) - \frac{\partial L}{\partial\beta} = Q_\beta$$

(2.14)

After performing the necessary operations in the above equation, the equation of motion for β is obtained as follows (see 2.15).

$$m_2 L_1 L_2 cos\beta\ddot\theta + \left(m_2 L_2{}^2 + I_2\right)\ddot\beta - m_2 L_2{}^2 sin\beta cos\beta\dot\theta^2 - m_2 g L_2 sin\beta = -b_2\dot\beta$$

(2.15)

If the expressions θ and β in the equations of motion are separated, the following equations are obtained (see 2.16 and 2.17).

$$\ddot\theta = \frac{\left(m_2 L_2{}^2 + I_2\right)\left(b_1\dot\theta - \tau - m_2 L_1 L_2 sin\beta\dot\beta^2 + 2m_2 L_2{}^2 sin\beta cos\beta\dot\beta\dot\theta\right)}{(m_2 L_1 L_2 cos\beta)^2 - \left(m_2 L_2{}^2 + I_2\right)\left(m_1 L_1{}^2 + I_1 + m_2 L_1 + m_2 L_2{}^2 sin^2\beta\right)}$$

$$- \frac{m_2 L_1 L_2 cos\beta\left(b_2\dot\beta - m_2 L_2{}^2 sin\beta cos\beta\dot\theta^2 - m_2 g L_2 sin\beta\right)}{(m_2 L_1 L_2 cos\beta)^2 - \left(m_2 L_2{}^2 + I_2\right)\left(m_1 L_1{}^2 + I_1 + m_2 L_1 + m_2 L_2{}^2 sin^2\beta\right)}$$

(2.16)

$$\ddot\beta = \frac{\left(m_1 L_1{}^2 + I_1 + m_2 L_1 + m_2 L_2{}^2 sin^2\beta\right)\left(b_2\dot\beta - m_2 L_2{}^2 sin\beta cos\beta\dot\theta^2 - m_2 g L_2 sin\beta\right)}{(m_2 L_1 L_2 cos\beta)^2 - \left(m_2 L_2{}^2 + I_2\right)\left(m_1 L_1{}^2 + I_1 + m_2 L_1 + m_2 L_2{}^2 sin^2\beta\right)}$$

$$- \frac{m_2 L_1 L_2 cos\beta\left(b_1\dot\theta - \tau - m_2 L_1 L_2 sin\beta\dot\beta^2 + 2m_2 L_2{}^2 sin\beta cos\beta\dot\beta\dot\theta\right)}{(m_2 L_1 L_2 cos\beta)^2 - \left(m_2 L_2{}^2 + I_2\right)\left(m_1 L_1{}^2 + I_1 + m_2 L_1 + m_2 L_2{}^2 sin^2\beta\right)}$$

(2.17)

The equation of motion of the DC motor that provides the rotational motion of the first arm can be written as follows (see 2.18). Here, V_a is the motor supply voltage and also the control signal, K_b is the back electromotive voltage coefficient, N is the gear ratio, R is the motor winding ohmic resistance, L is the motor inductance coefficient and i is the electrical current flowing through the motor windings.

$$\frac{di}{dt} = \frac{V_a - Ri}{L} - \frac{K_b\dot\theta}{LN}$$

(2.18)

If we convert the expressions in the equations into state variables is obtained as 2.19, 2.20, 2.21, 2.22 and 2.23:

$$\theta = x(1)$$ (2.19)
$$\dot\theta = x(2)$$ (2.20)
$$\beta = x(3)$$ (2.21)
$$\dot\beta = x(4)$$ (2.22)
$$\frac{di}{dt} = x(5)$$ (2.23)

The motor control torque is calculated as 2.24:

$$\tau = \frac{K_t i}{N}$$

(2.24)

Where is the motor torque coefficient.

For the rotary inverted pendulum system, using these state variables, the moving sliding mode control method was applied with the help of the program written in the Matlab program. With this control method, it will be ensured that the pendulum angle β goes to the desired zero reference point. The Values of used system parameters are given in table 1.

Table 1

System Parameter Values

Parameter	Value	Unit
m_1	0.15	kg
m_2	0.1	kg
L_1	0.4	m
L_2	0.4	m
b_1	0.01	Ns/m
b_2	0.01	Ns/m
I_1	0.0248	kgm2
I_2	0.00386	kgm2
L	0.1	Henry
R	1.4	Ohm
K_t	0.25	-
K_b	0.05	-
N	1/20	-

2.2 Sliding Surface Moving Fuzzy Sliding Mode Control Design

The sliding mode control method is a nonlinear and robust control method. Compared to other control methods, it is a method that is not affected by external disturbances. Thanks to the oscillations on the sliding surface to reach the desired reference, it can reach the result quickly with high accuracy (Young, Utkin, & Ozguner, 1999). Because the system parameters are unknown or constantly changing and there are external disturbances affecting the system, the sliding mode control allows long-term controllability as long as the limit values of the system are known.

While performing the sliding mode control design, the slip surface must first be determined and a control rule must be created to reach the determined slip surface. The time taken to reach the slip surface is called the reach time. This region of the phase trajectory is called the reach mode. In reach mode, the system is sensitive to parameter uncertainty and external noise (Edwards & Spurgeon, 1998). When the slip surface is reached, the slip mode starts, in which the trajectory of the system is insensitive to uncertain parameters and external factors. Chattering in sliding mode control applications is caused by oscillations around the system's desired equilibrium point, and it discloses the system's unmodeled high-frequency dynamics. Sliding mode control expression with sign function can be written as 2.25:

U = -k sign(S)

(2.25)

S in equation 25 is the slip surface function and it can be expressed as given in equation (2.26), depending on the error (e) that occurs according to the response of the system and the variation of the error with time (de). When choosing S, the slope of the slip surface C is taken as a time variable. The slope value is updated instantly by looking at the answers of the system.

$$S = C\,e + de \tag{2.26}$$

An example of the sliding surface of the sliding mode control is shown in figure 2. As can be seen from the given figure, the slip surface has a certain slope. The coefficient C in equation (2.26) represents this slope.
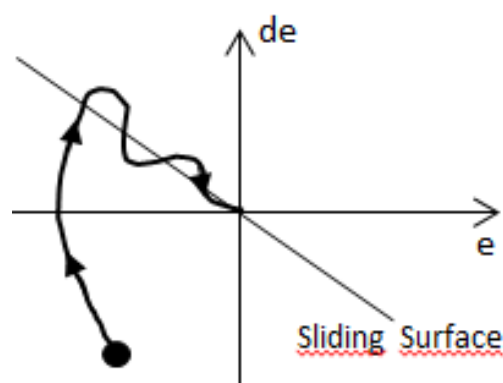
Figure 2. Sliding surface

The controller's success is ensured by determining the best value for this defined slope. The sliding mode controller's slip surface slope coefficients are treated as moving in this investigation. Fuzzy logic was used to calculate the slope coefficient C. Mamdani type was used as fuzzy inference method. Center of gravity was used as the defuzzification method. The error of the pendulum angle and the derivative of the pendulum error are given as an introduction to the fuzzy logic structure. As an output, the slope coefficient of the sliding surface of the sliding mode control is obtained. The optimum values of the base coefficients of the membership functions in the fuzzy logic structure were calculated using a genetic algorithm. Genetic algorithm parameters were used as FitnessLimit 1e-10, Generations 100 and PopulationSize 20. Figure 3 shows the block diagram in which the coefficients of the controller are optimized by the genetic algorithm technique.
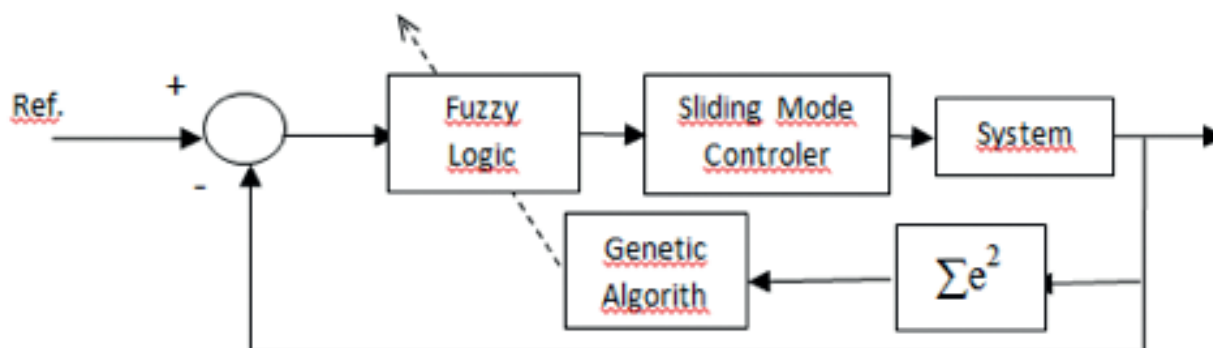

Figure 3. Controller Block Diagram

Since the C coefficient obtained will vary each time, the control method has a moving sliding surface. Below is the Figure 4 showing the mobility of the C coefficient.
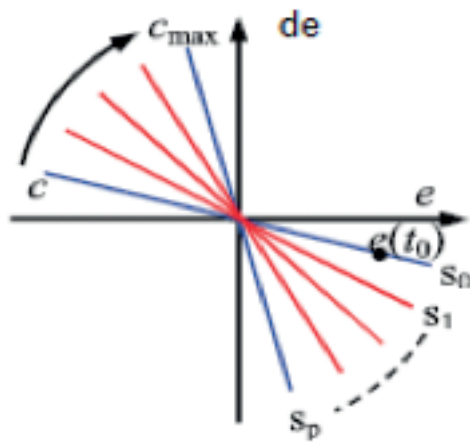

Figure 4. Variation of the C coefficient

The rule table for the inputs and the output for the fuzzy logic structure, membership functions are shown in table 2, figure 5, figure 6, and figure 7, respectively. Triangular membership functions are used for each input and output.

Table 2

Rule table of fuzzy logic structure for slip surface C

e \ de/dt	NB_{de}	Z_{de}	PB_{de}
NB_e	Z	NB	NB
Z_e	NB	Z kg	PB
PB_1	PB	PB	PB
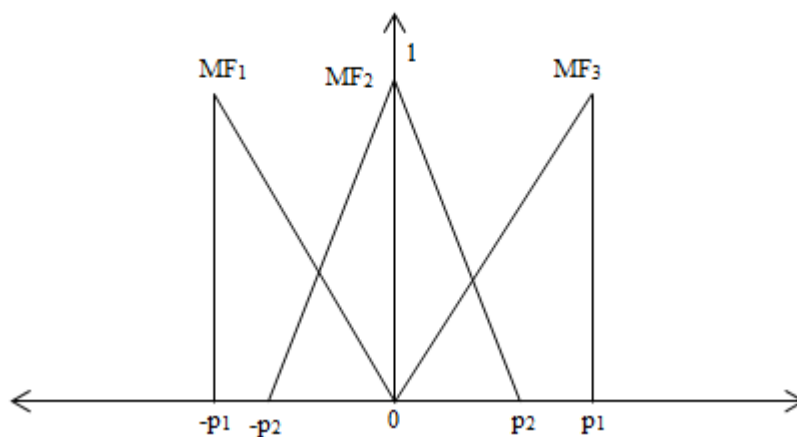
Figure 5. Membership functions for input1(e)
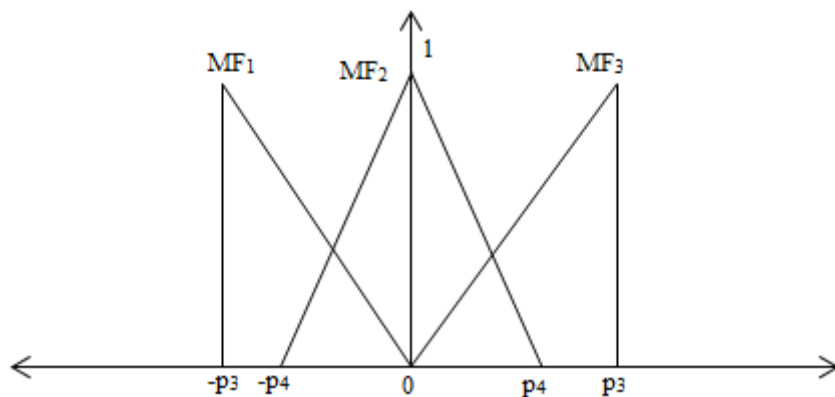
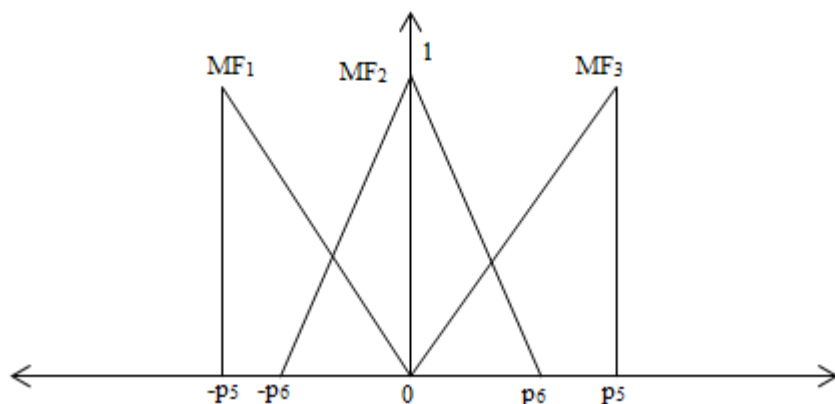Figure 6. Membership functions for input2(de/dt)

Figure 7. Membership functions for output (C)

The p_1, p_2, p_3, p_4, p_5, and p_6 values of the base coefficients of the membership functions used in the fuzzy structures were calculated by genetic algorithm and obtained as given in table 3

Table 3

Base values of membership functions

p_1	p_2	p_3	p_4	p_5	p_6
20.7646	0.4166	0.7657	11.0061	91.7301	8.4752

The sign function in the sliding mode control expression causes the control signal to crackle. Various types of functions are used instead of this sign function to solve this problem. The widely used saturation function was chosen to replace the sign function in this study. As a result, equation (2.27) calculates the sliding mode control expression with saturation function.

$$U = -k*SAT(S / epsilon) \qquad\qquad (2.27)$$

Where the epsilon value was found to be 74.55 by genetic algorithm. The Fitness value-Generation (Iteration) graph of the optimization process performed while calculating the unknown coefficients with the genetic algorithm is given in figure 8.

3. Results and Discussion

In figure 9, the variation of the angular position of the first arm connected to the motor with respect to time is seen. It started from the zero point at the beginning and changed direction in the first seconds. This is an expected result to raise the pendulum.
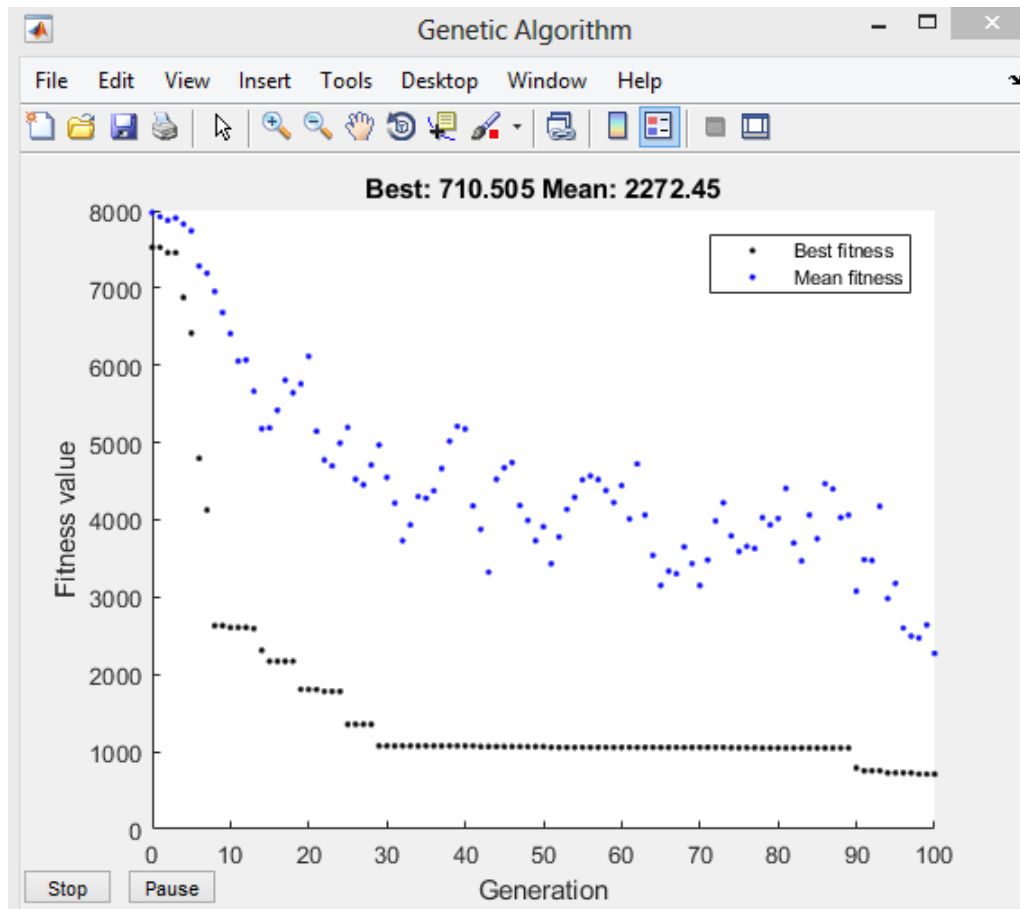
362

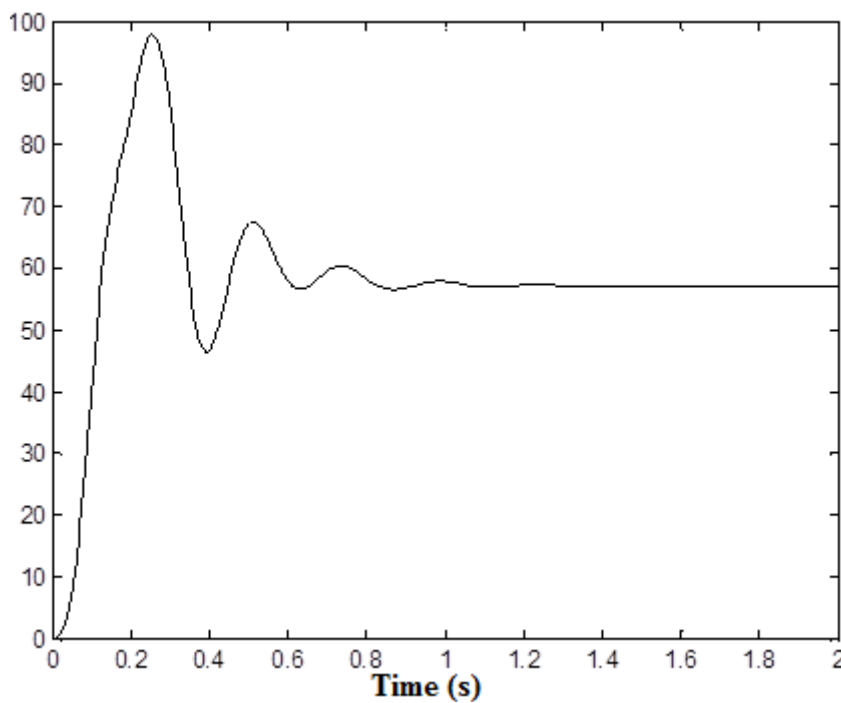Figure 8. The Fitness value-Generation (Iteration) graph of the genetic algorithm optimization process

Figure 9. Variation of theta angle according to time

The graph in figure 10 shows the angular velocity of the first arm to time. It is seen that the angular velocity value reaches 14 rad/s at the beginning and is fixed at 0 rad/s.
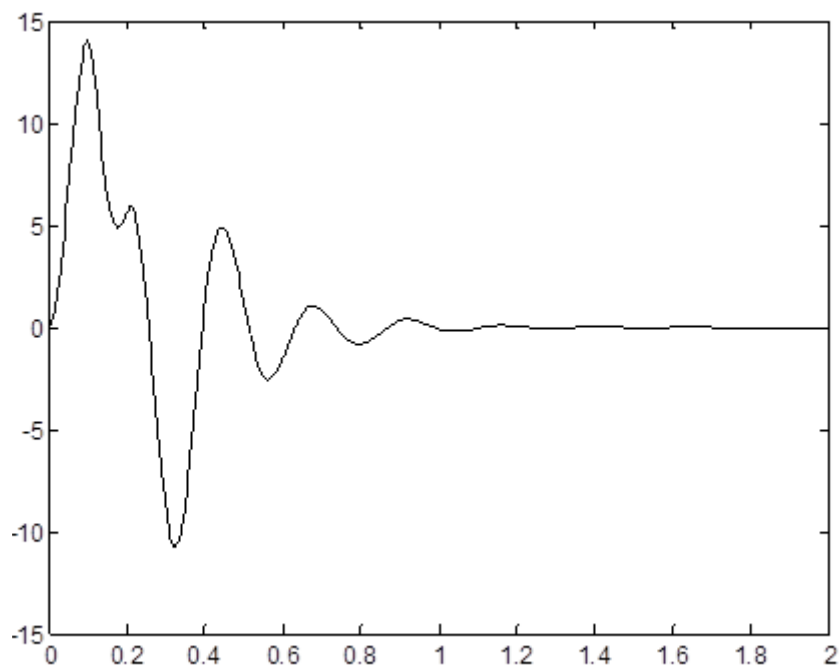
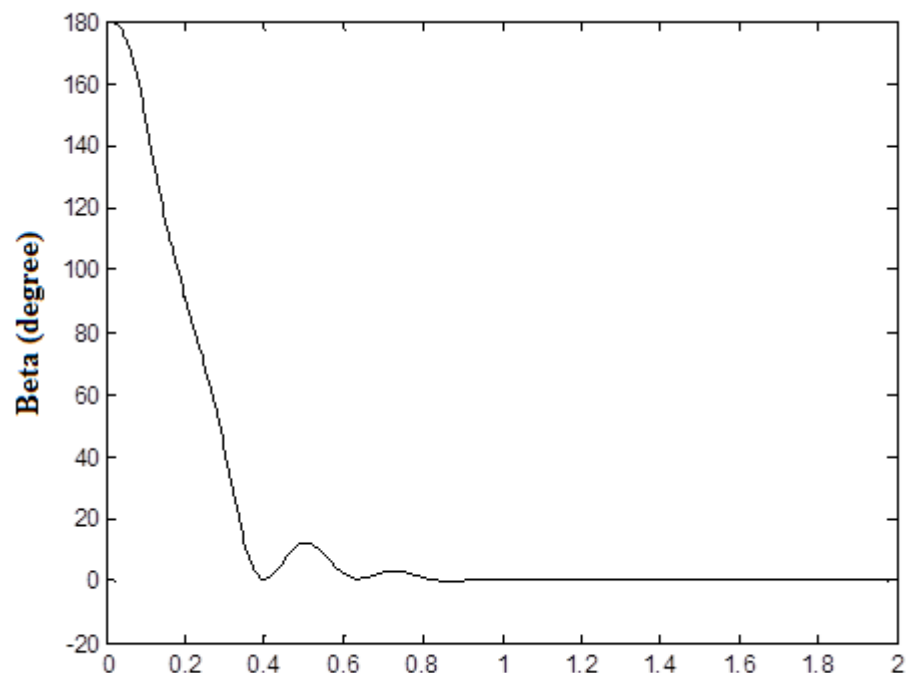Figure 10. Angular velocity change of the first arm according to time

Figure 11. Variation of beta angle (pendulum angle) according to time

In figure 11, there is a graph showing the change of pendulum angle with respect to time. The pendulum is required to stop at the unstable upper balance point. Therefore, the pendulum angle must reach the desired zero reference point. As seen in the figure, the pendulum reaches the desired reference value in about 1 second.

In figure 12, the variation of the angular velocity of the pendulum with time is shown. As can be seen from the graph, the angular velocity of the pendulum reaches zero after 1 second.
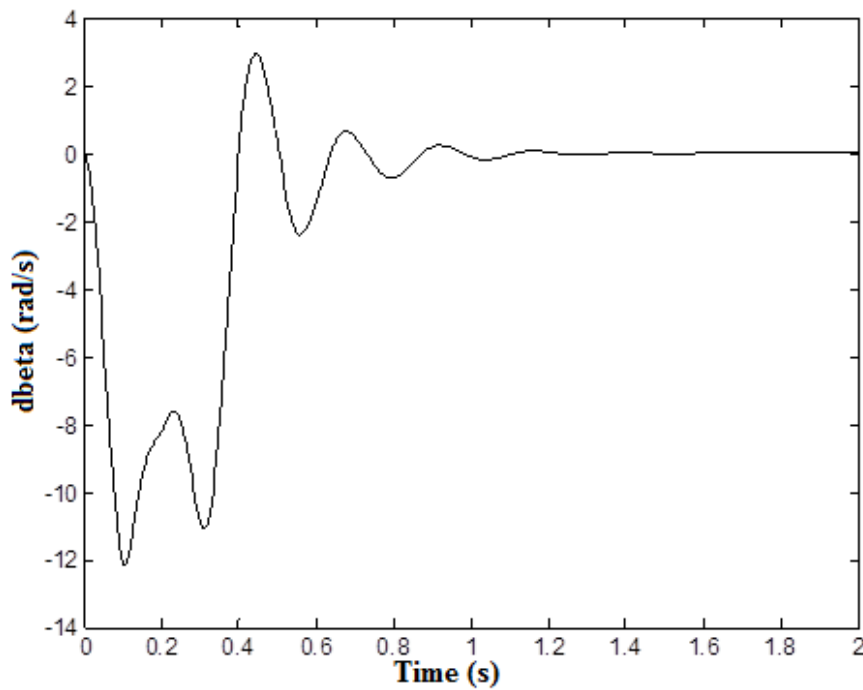
Figure 12. Angular velocity change of the pendulum according to time

In figure 13 and 14, respectively, the torque value of the DC motor to be applied to the first arm and the graph of the slope values of the slip surface are given. When the DC motor torque graph in figure 13 is examined, it is clear that approximately 20 Nm of motor torque will be sufficient to bring the pendulum to the desired reference value. It can be said that this torque value is reasonable for real applications. After about 1 second, the control signal reaches zero. When the slip surface slope graph in figure 14. is examined, it is seen that it takes values between 0-50 values.
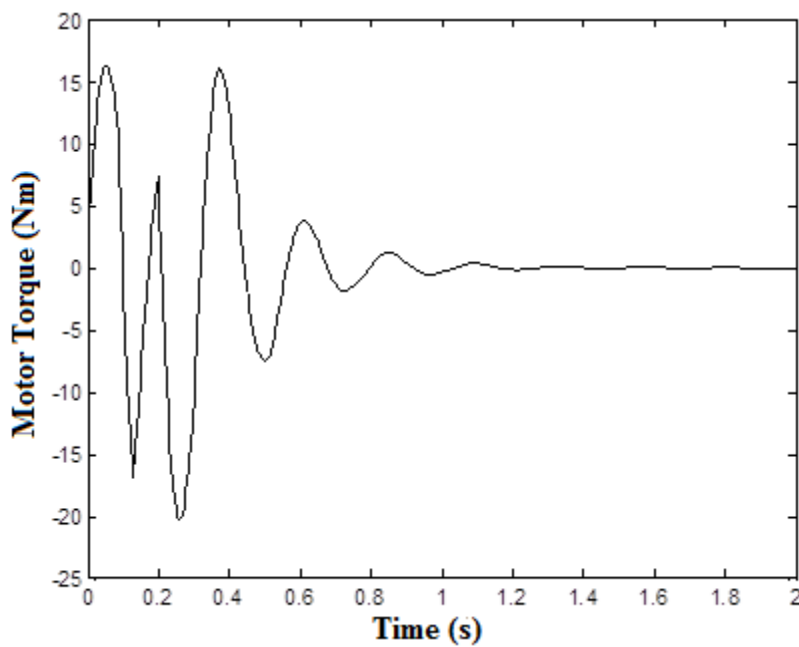

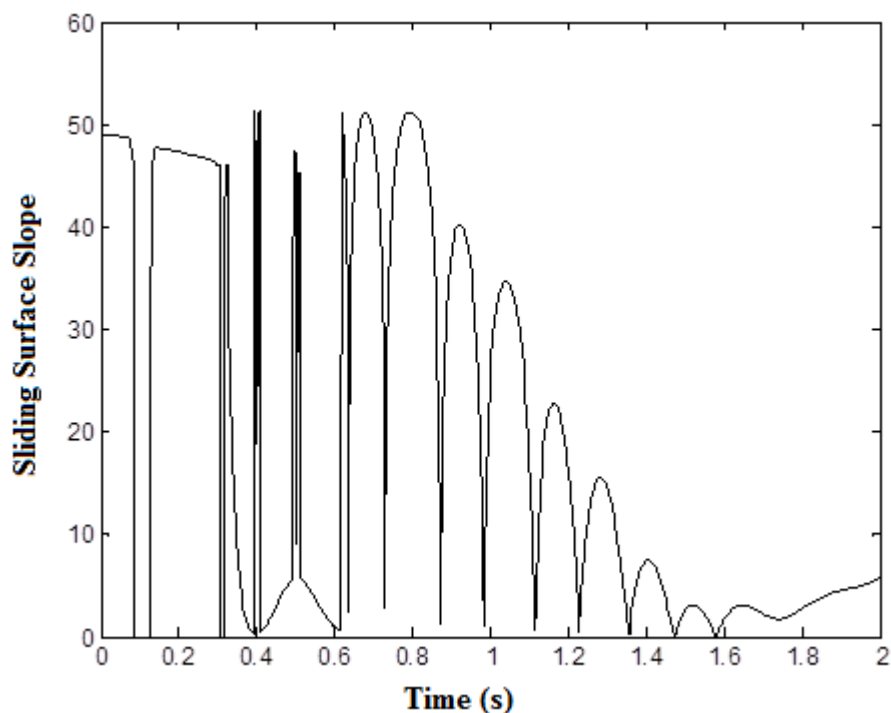Figure 13. Variation of DC motor's torque according to time

Figure 14. Sliding surface slope graph

Figure 15 shows the time variation of the supply voltage signal that should be applied to the DC motor. It can also be seen from the graph that the DC motor supply voltage source is limited to 12 volts. In figure 16, the variation of the current passing through the DC motor windings with time is shown. It is seen that the current drawn by the motor reaches zero value after about 1 second.
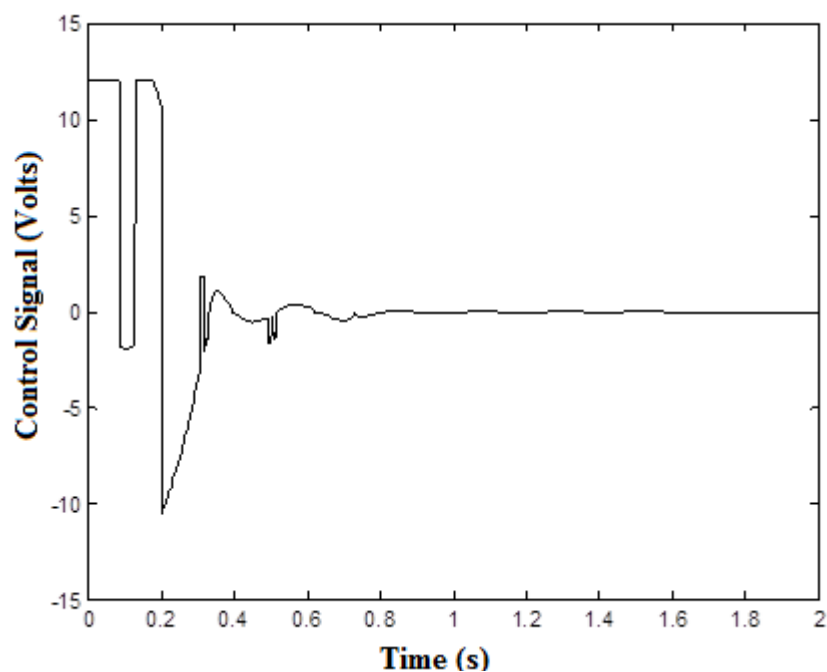

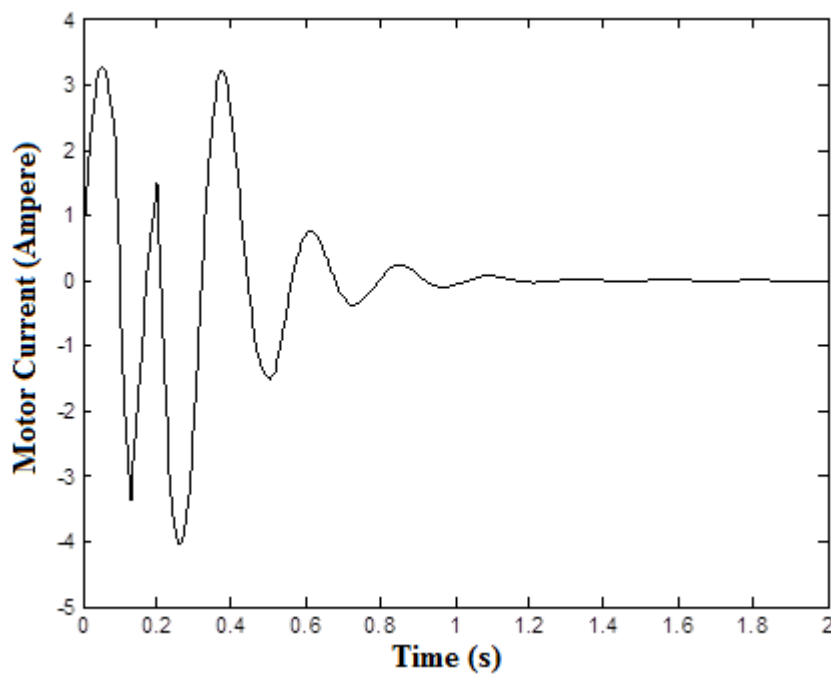Figure 15. Graph of DC Motor Control Signal according to Time

Figure 16. Graph of DC Motor Current according to Time

In Table 4, the results of the study conducted in this research article and a publication in the literature are compared. As can be seen in the table, the pendulum angle of the system achieved a better settling time of 0.9 s in the current study (Nath & Dewan 2018)..

Table 4

Comparison of between work in the literature and the present work

	Method	Settling Time (s)	Max. Overshoot (rad)	Max. Undershoot (rad)
Rotary inverted pendulum arm angle results	LQR	0.80	0.1260	-
	SMC	0.80	0.1460	-
	Present Work	1.05	0.6981	0.1523
Pendulum angle results	LQR	1.25	0.0072	- 0.003
	SMC	1.25	0.0130	- 0.004
	Present Work	0.90	0.1745	- 0.035

4. Conclusion

In this study, the nonlinear model of the rotary inverted pendulum system, which has a single degree of freedom, was first obtained using the Lagrangian method. The pendulum angle was controlled by the program created in Matlab with the help of state variables on the model obtained. For this reason, the system has been controlled using the moving sliding mode control approach. The variability of the slope of the slip surface was calculated by the fuzzy logic method. The coefficients of the fuzzy logic structure were calculated with the help of the genetic algorithm. At the end of the study, it was observed that the pendulum reached the desired reference value in about 1 second, the error was zero, and the control signal reached zero. It has been observed that the motor torque value reaches up to 20 Nm and the motor draws a maximum of 4 amperes. From these results, it has been obtained that the moving sliding mode control can be applied to the system without any problems if the motor is selected considering the obtained motor values in the real-time motor selection.

Author Contributions

Muhammet Aydin: Modeling of rotary inverted pendulum system.

Oğuz Yakut: Sliding surface moving fuzzy sliding mode control design.

Conflicts of Interest

The authors declare no conflict of interest.

References

Altinoz, O. T., Yilmaz, A. E., & Weber, G. W. (2010). Chaos particle swarm optimized PID controller for the inverted pendulum system. In *2nd international conference on engineering optimization*. http://www.dem.ist.utl.pt/engopt2010/Book_and_CD/Papers_CD_Final_Version/pdf/01/01454-01.pdf

Awtar, S., King, N., Allen, T., Bang, I., Hagan, M., Skidmore, D., & Craig, K. (2002). Inverted pendulum systems: rotary and arm-driven-a mechatronic system design case study. *Mechatronics*, *12*(2), 357-370. https://doi.org/10.1016/S0957-4158(01)00075-7

Aydin, M., Yakut, O., & Tutumlu, H. (2019). Implementation of the Network-Based Moving Sliding Mode Control Algorithm to the Rotary Inverted Pendulum System. *Journal of Engineering and Technology*, *3*(1), 32-41. https://dergipark.org.tr/en/download/article-file/721111

Bogdanov, A. (2004, Aralık) Optimal control of a double inverted pendulum on a cart, Health and Science University Technical Report.

Bugeja, M. (2003, September). Non-linear swing-up and stabilizing control of an inverted pendulum system. In *The IEEE Region 8 EUROCON 2003. Computer as a Tool.* (Vol. 2, pp. 437-441). IEEE. https://doi.org/10.1109/EURCON.2003.1248235

Chawla, I., & Singla, A. (2021). Real-Time Stabilization Control of a Rotary Inverted Pendulum Using LQR-Based Sliding Mode Controller. Arabian Journal for Science and Engineering, 46(3), 2589-2596. https://doi.org/10.1007/s13369-020-05161-7

Cui, J. (2019, July). Numerical Design Method for Nonlinear Sliding Mode Control of Inverted Pendulum. In 2019 Chinese Control Conference (CCC) (pp. 2646-2649). IEEE. http://doi.org/10.23919/ChiCC.2019.8865123

Edwards, C., & Spurgeon, S. (1998). *Sliding mode control: theory and applications*. Crc Press.

Hassanzadeh, I., & Mobayen, S. (2008). PSO-based controller design for rotary inverted pendulum system. *Journal of Applied Sciences*, *8*(16), 2907-2912. https://docsdrive.com/pdfs/ansinet/jas/2008/2907-2912.pdf

Hazem, Z. B., Fotuhi, M. J., & Bingül, Z. (2020). A comparative study of the joint neuro-fuzzy friction models for a triple link rotary inverted pendulum. Ieee Access, 8, 49066-49078. http://doi.org/10.1109/ACCESS.2020.2978025

Hazem, Z. B., Fotuhi, M. J., & Bingül, Z. (2020). Development of a Fuzzy-LQR and Fuzzy-LQG stability control for a double link rotary inverted pendulum. Journal of the Franklin Institute, 357(15), 10529-10556. https://doi.org/10.1016/j.jfranklin.2020.08.030

Hong, G. B., Nguyen, H. T., Nguyen, M. T., Hoang Le, T. T., & Hai Nguyen, V. D. (2019). TRAJECTORY TRACKING FOR FUTURA PENDULUM BY INCREMENTAL SLIDING MODE CONTROL. Robotica & Management, 24(1). https://web.p.ebscohost.com/ehost/pdfviewer/pdfviewer?vid=0&sid=6590e51f-2bfb-4b30-b7aa-5aa088f805fc%40redis

Howimanporn, S., Chookaew, S., & Silawatchananai, C. (2020, October). Comparison between PID and Sliding Mode Controllers for Rotary Inverted Pendulum Using PLC. In 2020 4th International Conference on Automation, Control and Robots (ICACR) (pp. 122-126). IEEE. http://doi.org/10.1109/ICACR51161.2020.9265510

Khanesar, M. A., Teshnehlab, M., & Shoorehdeli, M. A. (2007, June). Sliding mode control of rotary inverted pendulm. In *2007 Mediterranean Conference on Control & Automation* (pp. 1-6). IEEE. https://doi.org/10.1109/MED.2007.4433653

Krishen, J., & Becerra, V. M. (2006, October). Efficient fuzzy control of a rotary inverted pendulum based on LQR mapping. In *2006 IEEE Conference on Computer Aided Control System Design, 2006 IEEE International Conference on Control Applications, 2006 IEEE International Symposium on Intelligent Control* (pp. 2701-2706). IEEE. https://doi.org/10.1109/CACSD-CCA-ISIC.2006.4777066

Kuo, T. C., Huang, Y. J., & Hong, B. W. (2009, July). Adaptive PID with sliding mode control for the rotary inverted pendulum system. In *2009 IEEE/ASME International Conference on Advanced Intelligent Mechatronics* (pp. 1804-1809). IEEE. http://doi.org/10.1109/AIM.2009.5229784

Le, T. T. H., Vo, A. K., Van Nguyen, T., Vu, D. H., & Tran, M. S. (2018). FUZZY CONTROLLER FOR ROTARY INVERTED PENDULUM. Robotica & Management, 23(2). https://web.p.ebscohost.com/ehost/pdfviewer/pdfviewer?vid=2&sid=0f28d825-27ec-4362-a82b-dd944bf02a20%40redis

Muñoz-Poblete, C. (2018, October). Pole placement controller applied to a Rotary Inverted Pendulum System. A didactic view. In 2018 IEEE International Conference on Automation/XXIII Congress of the Chilean Association of Automatic Control (ICA-ACCA) (pp. 1-6). IEEE. http://doi.org/10.1109/ICA-ACCA.2018.8609824

Nath, K., & Dewan, L. (2017, November). Control of a rotary inverted pendulum via adaptive techniques. In 2017 International Conference on Emerging Trends in Computing and Communication Technologies (ICETCCT) (pp. 1-6). IEEE. http://doi.org/10.1109/ICETCCT.20178280315

Nath, K., & Dewan, L. (2018, March). A comparative analysis of linear quadratic regulator and sliding mode control for a rotary inverted pendulum. In 2018 International Conference on Recent Trends in Electrical, Control and Communication (RTECC) (pp. 302-307). IEEE. http://doi.org/10.1109/RTECC.2018.8625648

Stimac, A. K. (1999). *Standup and stabilization of the inverted pendulum* (Doctoral dissertation, Massachusetts Institute of Technology, Dept. of Mechanical Engineering). https://ocw.mit.edu/courses/mechanical-engineering/2-003-modeling-dynamics-and-control-i-spring-2005/study-materials/andrew.pdf

Sugie, T., & Fujimoto, K. (1998). Controller design for an inverted pendulum based on approximate linearization. *International Journal of Robust and Nonlinear Control: IFAC-Affiliated Journal*, *8*(7), 585-597. https://doi.org/10.1002/(SICI)1099-1239(199806)8:7<585::AID-RNC331>3.0.CO;2-B

Sukontanakarn, V., & Parnichkun, M. (2009). Real-time optimal control for rotary inverted pendulum. *American journal of applied sciences*, *6*(6), 1106. http://citeseerx.ist.psu.edu/viewdoc/download?doi=10.1.1.1020.5634&rep=rep1&type=pdf

Wang, W. (2009). Adaptive fuzzy sliding mode control for inverted pendulum. In *Proceedings. The 2009 International Symposium on Computer Science and Computational Technology (ISCSCI 2009)* (p. 231). Academy Publisher. https://citeseerx.ist.psu.edu/viewdoc/download?doi=10.1.1.648.7484&rep=rep1&type=pdf

Yan, Q. (2003, December). Output tracking of underactuated rotary inverted pendulum by nonlinear controller. In *42nd IEEE International Conference on Decision and Control (IEEE Cat. No. 03CH37475)* (Vol. 3, pp. 2395-2400). IEEE. http://doi.org/10.1109/CDC.2003.1272978

Yiğit, İ. (2017). Model free sliding mode stabilizing control of a real rotary inverted pendulum. Journal of Vibration and Control, 23(10), 1645-1662. https://doi.org/10.1177/1077546315598031

Young, K. D., Utkin, V. I., & Ozguner, U. (1999). A control engineer's guide to sliding mode control. *IEEE transactions on control systems technology*, *7*(3), 328-342. http://doi.org/10.1109/87.761053

Zhong, W., & Rock, H. (2001, September). Energy and passivity based control of the double inverted pendulum on a cart. In *Proceedings of the 2001 IEEE International Conference on Control Applications (CCA'01)(Cat. No. 01CH37204)* (pp. 896-901). IEEE. http://doi.org/10.1109/CCA.2001.973983

Zabihifar, S. H., Yushchenko, A. S., & Navvabi, H. (2020). Robust control based on adaptive neural network for Rotary inverted pendulum with oscillation compensation. Neural Computing and Applications, 32(18), 14667-14679. https://doi.org/10.1007/s00521-020-04821-x